Amino Acids (2015) 47:719–727
DOI 10.1007/s00726-014-1899-4

ORIGINAL ARTICLE

Synthesis and preliminary biological evaluation of *S*-^{11}C-methyl-D-cysteine as a new amino acid PET tracer for cancer imaging

Tingting Huang · Ganghua Tang · Hongliang Wang · Dahong Nie · Xiaolan Tang · Xiang Liang · Kongzhen Hu · Chang Yi · Baoguo Yao · Caihua Tang

Received: 18 September 2014 / Accepted: 9 December 2014 / Published online: 23 December 2014

Abstract *S*-^{11}C-methyl-L-cysteine (LMCYS) is an attractive amino acid tracer for clinical tumor positron emission tomography (PET) imaging. D-isomers of some radiolabeled amino acids are potential PET tracers for tumor imaging. In this work, *S*-^{11}C-methyl-D-cysteine (DMCYS), a D-amino acid isomer of *S*-^{11}C-methyl-cysteine for tumor imaging was developed and evaluated. DMCYS was prepared by ^{11}C-methylation of the precursor D-cysteine, with an uncorrected radiochemical yield over 50 % from $^{11}CH_3I$ within a total synthesis time from $^{11}CO_2$ about 12 min. In vitro competitive inhibition studies showed that DMCYS uptake was primarily transported through the Na^+-independent system L, and also the Na^+-dependent system $B^{0,+}$ and system ASC, with almost no system A. In vitro incorporation experiments indicated that almost no protein incorporation was found in Hepa 1–6 hepatoma cell lines. Biodistribution studies demonstrated higher uptake of DMCYS in pancreas and liver at 5 min post-injection, relatively lower uptake in brain and muscle, and faster radioactivity clearance from most tissues than those of L-isomer during the entire observation time. In the PET imaging of S180 fibrosarcoma–bearing mice and turpentine-induced inflammatory model mice, 2-^{18}F-fluoro-2-deoxy-D-glucose (FDG) exhibited significantly high accumulation in both tumor and inflammatory lesion with low tumor-to-inflammation ratio of 1.40, and LMCYS showed low tumor-to-inflammation ratio of 1.64 at 60 min post-injection. By contrast, DMCYS showed moderate accumulation in tumor and very low uptake in inflammatory lesion, leading to relatively higher tumor-to-inflammation ratio of 2.25 than ^{11}C-methyl-L-methionine (MET) (1.85) at 60 min post-injection. Also, PET images of orthotopic transplanted glioma models demonstrated that low uptake of DMCYS in normal brain tissue and high uptake in brain glioma tissue were observed. The results suggest that DMCYS is a little better than the corresponding L-isomers as a potential PET tumor-detecting agent and is superior to MET and FDG in the differentiation of tumor from inflammation.

Keywords Amino acid transporter · Tumor · PET imaging · *S*-^{11}C-methyl-D-cysteine

Introduction

2-^{18}F-Fluoro-2-deoxy-D-glucose (FDG) is the most widely used radiopharmaceutical for detection of tumor and monitoring response to therapy (Kumar et al. 2010; Plathow and Weber 2008). However, clinical FDG positron emission tomography (PET) studies have demonstrated several limitations, such as a high uptake in normal tissue of the brain and in inflammatory tissues (Kubota et al. 1994), which is a major cause of false-positive results. Furthermore, as not all tumor types display increased uptake of FDG, imaging strategies targeting other metabolic functions of tumors are required to improve diagnosis and management of cancer patients.

Radiolabeled amino acids have been studied as potential PET tracers for clinical tumor imaging, especially for detection of brain cancer (Jager et al. 2001). Their use in

T. Huang · G. Tang (✉) · H. Wang · D. Nie · X. Liang · K. Hu · C. Yi · B. Yao · C. Tang
Department of Nuclear Medicine, The First Affiliated Hospital, Sun Yat-Sen University, Guangzhou 510080, China
e-mail: gtang0224@126.com

X. Tang
Department of Applied Chemistry, South China Agricultural University, Guangzhou 510642, China
e-mail: tangtxl1972@163.com

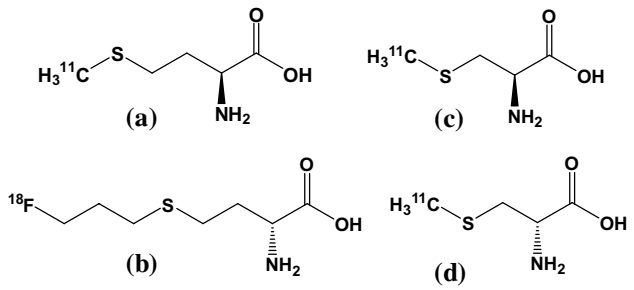

Fig. 1 Structures of **a** *S*-^{11}C-methyl-L-methionine (MET), **b** *S*-(3-[^{18}F]fluoropropyl)-D-homocysteine (DFPHCys), **c** *S*-^{11}C-methyl-L-cysteine (LMCYS) and **d** *S*-^{11}C-methyl-D-cysteine (DMCYS)

tumor detection is based primarily on an increased cellular uptake of amino acids, which is assumed to reflect an enhanced amino acid transport and protein synthesis. The most frequently used amino acid PET tracer is *S*-^{11}C-methyl-L-methionine (MET, Fig. 1a) because of its easy and fast radiosynthesis in the hospitals with an on-site cyclotron (Langstrom et al. 1987). It demonstrates an enormous potential for PET imaging of brain tumor (Okubo et al. 2010) and prostate cancer (Nunez et al. 2002). However, increased nonspecific uptake of MET in malignant tumors is found by some investigators in many clinical PET studies (Kubota 2001; Sasaki et al. 2001; Yasukawa et al. 2000) and some inflammatory lesions also take up MET (Maeda et al. 2003). It has been reported that MET is not only a substrate for transport and protein synthesis, but also is involved into polyamine synthesis and transmethylation reactions, which complicates quantitative imaging of protein synthesis (Deng et al. 2011). Moreover, though *O*-2-^{18}F-fluoroethyl-L-tyrosine (FET) with longer half-life of ^{18}F is another commonly used ^{18}F-labeled amino acid for the detection of tumors with superior to FDG in distinguishing tumor from inflammation (Lee et al. 2009), it is cumbersome and time-consuming for the automated radiosynthesis of FET with complex high-performance liquid chromatography (HPLC) purification (Hamacher and Coenen 2002) compared with the simple production of MET by on-column methylation (Pascali et al. 1999). Therefore, the easy availability of ^{11}C-methyl–containing tracers in the PET center with an in-house cyclotron makes its potential use in clinical PET imaging.

Our previous study found *S*-^{11}C-methyl-L-cysteine (LMCYS, Fig. 1c), an analog of MET, was superior to FDG and MET in the differentiation of tumor from inflammation (Deng et al. 2011). Because L-isomers of amino acids are commonly used for protein synthesis in mammalian cells in nature, D-isomers are considered to be unnatural amino acids which exhibit almost no incorporation into the protein fraction and relatively low accumulation in inflammatory tissues, with no significant elevation of the radioactivity in normal peripheral tissues over time. It has been reported that D-isomers of some radiolabeled PET amino acids, such as *O*-^{11}C-methyl-D-tyrosine (DCMT) and *O*-^{18}F-fluoromethyl-D-tyrosine (DFMT) (Tsukada et al. 2006b), *O*-^{18}F-fluoroethyl-D-tyrosine (DFET) (Tsukada et al. 2006a; Urakami et al. 2009), and *S*-(3-[^{18}F]fluoropropyl)-D-homocysteine (DFPHCys, Fig. 1b) (Bourdier et al. 2011; Denoyer et al. 2012), are more potential PET tracers than the corresponding L-isomers for tumor imaging.

The objectives of the present work were to radiolabel the D-isomer of MCYS with ^{11}C (*S*-^{11}C-methyl-D-cysteine, DMCYS, Fig. 1d) and evaluate potential value of this new amino acid imaging agent in comparison with its corresponding L-isomer as well as MET in tumor-bearing mice.

Materials and methods

Chemicals

All reagents, unless otherwise specified, were of analytical grade and commercially available. Dimethylsulfoxide (DMSO), acetonitrile (MeCN), tetrahydrofuran (THF), *N*, *N*-dimethylformamide (DMF), lithium aluminum hydride (1.0 M in tetrahydrofuran), hydroiodic acid, L- and D-cysteine, and L-MET were purchased from Sigma–Aldrich (Milwaukee, WI, USA). L- and D-isomers of MCYS were synthesized by reactions of methyl iodide with the corresponding L- and D-cysteine.

Cell culture and animal models

The Hepa1–6 hepatocellular carcinoma cell lines, the S180 fibrosarcoma cells, and the female Kunming mice (6 weeks old) were obtained from the Laboratory Animal Center of Sun Yat-Sen University (Guangzhou, China). The Hepa1–6 cells were used for the in vitro experiments of the transport assay and protein incorporation. The cells were cultivated in RPMI 1640 medium with a physiologic glucose concentration (1.0 g/L) containing 5 % fetal calf serum at 37 °C in a humidified atmosphere of 5 % CO_2 and 95 % air. The medium was routinely renewed three times a week. Two days before the in vitro experiments, the Hepa1–6 cells were trypsinized and 2×10^5 cells per well were seeded into 24-well plates.

We prepared three groups of mice, namely 40 normal mice for biodistrubution studies of DMCYS or LMCYS ($n = 4$ for each time point in total five time points), 20 tumor-bearing mice for PET imaging with DMCYS or LMCYS or LMET or FDG, and 20 inflammation mice for PET imaging. For the in vivo studies, twenty mice were subcutaneously injected into the right shoulder with a 0.2 mL suspension containing 2×10^7 S180 fibrosarcoma

cells, maintained for 2–3 weeks after xenotransplantation while monitoring the growth rate, and subjected to experiments at 8–9 weeks of age. Inflammation mice were obtained through intramuscular injection into the thigh muscle with 0.2 mL of turpentine oil in 72 h (Yamada et al. 1995) before injection of the PET tracers. These turpentine-induced masses showed chronic inflammation histologically as described in an earlier report (Yamada et al. 1995). The mass of the tumors and inflammatory tissue grew to about 0.6–1.0 cm during the experiments. The mice were housed five animals per cage under standard laboratory conditions at 25 °C and 50 % humidity and allowed free access to food and water. At the time of the experiments, the mice were weighed 25–32 g. The study was performed according to the guidelines and recommendations of the Committee on Animal Research at the First Affiliated Hospital, Sun Yat-Sen University. The protocol was fully approved by the local institutional review committee on animal care.

Syntheses of labeled compounds

$^{11}CO_2$ was produced by $^{14}N(p, \alpha)^{11}C$ nuclear reactions using a Cyclone 10/5 cyclotron (IBA) and was delivered to the radiochemical laboratory. $^{11}CO_2$ was trapped in a loop ring cooled with liquid nitrogen. $^{11}CH_3I$ was prepared from reduction of $^{11}CO_2$ with $LiAlH_4$, hydrolysis of the intermediately formed organometallic complex, and subsequent iodination of ^{11}C-methanol with hydrogen iodide (Deng et al. 2011). DMCYS was synthesized according to the solid-phase ^{11}C-methylation of the precursor D-cysteine loaded into a C18 column with $^{11}CH_3I$ similar to the production of LMCYS (Deng et al. 2011). Briefly, $^{11}CH_3I$ was delivered under helium flow (20 ml/min) to a reaction vessel previously loaded with a solution of D-cysteine (about 2–3 mg) dissolved in 0.5 mol/L NaOH solution in 50:50 ethanol: water (v/v, 0.210 mL). After reaction, DMCYS was eluted with NaH_2PO_4 0.05 mol/L buffer (5 mL, pH 3–4). The eluents were collected in a vented sterile vial through a 0.22 μm sterile filter. LMCYS, MET and FDG were synthesized as previously published by Tang et al. (Deng et al. 2011; Tang et al. 2004, 2006).

In vivo biodistribution studies

40 normal animals were injected with 1.48–2.96 MBq (40–80 μCi) of DMCYS or LMCYS ($n = 20$ each tracer) in 100–200 μL of phosphate-buffered saline (PBS) through the tail vein. They were anesthetized with 10 % chloral hydrate solution (3 mL/kg) before injection of radiotracer and remained anesthetized through the study. At 5, 15, 30, 45, and 60 min post-injection of the radiotracer, the mice ($n = 5$ per each time point) were sacrificed by cervical fracture and dissected. Blood was obtained through the eyeball, tissue samples of interest (blood, brain, heart, lung, liver, pancreas, kidney, stomach, small intestine, and muscle in the right thigh) were rapidly dissected and weighed, and ^{11}C radioactivity was counted with a gamma (γ) counter (GC-1200, USTC Chuangxin Co. Ltd. Zonkia Branch, China). All measurements were background-subtracted and decay-corrected to the sacrificed time and then averaged. Data were expressed as a percentage of the injected dose per gram of tissue (%ID/g).

Transport assays

The method of measuring transport was similar to a method reported previously (Langen et al. 2002, 2003; Urakami et al. 2009). Transport assays with Hepa l–6 cells were performed at 2-d after seeding during the exponential growth phase. To characterize the transport system were performed in the presence of the specific competitive inhibitors: 2-amino-2-norbornanecarboxylic acid (BCH) for system L; *N*-methyl-2-amino-isobutyric acid (MeAIB) for system A; and serine for system ASC. The concentration of the inhibitors used was 15 mmol/L. Parallel experiments with increasing concentrations of DMCYS were performed to investigate the capacity of the transport system. All experiments were performed in the presence and absence of Na^+. In Na^+-free experiments, sodium salts were replaced by choline chloride. Each experiment was done in triplicate and averaged and was repeated five times on different days. After preincubation of the cells in 200 μL of the medium for 30 min, 200 μL of DMCYS (1.85 MBq/mL) and 200 μL of one of the inhibitors or DMCYS (50, 100, 200, 300, or 350 μmol/L) were added and samples were incubated at 37 °C for 4 min. After tracer uptake had been stopped with 1 mL of ice-cold PBS, the cells were washed three times with phosphate-buffered saline at 4 °C and dissolved in 1.5 mL of 0.1 M NaOH plus 2 % Triton X (Sigma Chemical Co.) and the activity measured by γ counter.

Incorporation of DMCYS into proteins

The method of determining the extent of protein incorporation of DMCYS was performed according to the similar method reported elsewhere (Urakami et al. 2009). For incorporation of DMCYS into proteins experiments, the samples were respectively, incubated with 400 μL DMCYS at 37 °C for 30 min. At the end of incubation, the radioactive medium was removed. The cells were washed thrice with ice-cold PBS (1.0 mL, pH 7.4) and detached with 0.5 mL ethylenediaminetetraacetic acid (1 %), transferred into a cup and 0.5 mL 20 % trichloroacetic acid (TCA) was added. After 10 min on ice, the samples were centrifuged at 10,000 rpm for 4 min. The supernatant was removed, and

the pellet was washed three times with ice-cold PBS. The radioactivities in both the supernatant and the pellet were measured by a γ counter. Protein incorporation was calculated as the percentage of acid precipitable radioactivity.

PET studies

PET imaging was performed using a Gemini GXL-16 scanner (Philips, Dutch). Before underwent DMCYS, LMCYS, MET, and FDG PET studies, the animals were kept fasting for at least 4 h. The fibrosarcoma-bearing mice and inflammation model mice were anesthetized with 10 % chloral hydrate solution (3 mL/kg) before injection of the radiotracer and remained anesthetized throughout the study. DMCYS, LMCYS, MET, and FDG 1.48–2.96 MBq (40–80 μCi) were respectively, injected in 100–200 μL of PBS or normal saline through the tail vein. Then, image acquisition was performed at 45 (the best optimal PET scan time for ^{11}C labeled tracers) or 60 min (the best optimal PET scan time for ^{18}F-labeled tracers) after intravenous injection in 3-dimensional mode, with emission scans of 10 min per bed position. Imaging started with a low-dose CT scan (30 mAs), immediately followed by a PET scan. The CT scan was used for attenuation correction and localization of the lesion site.

After PET imaging at 60-min post-injection, the animals mentioned above were sacrificed, and tumor, inflammation tissues, muscle, and blood were excised. The tissue samples were weighed and the radioactivity was determined with a γ counter.

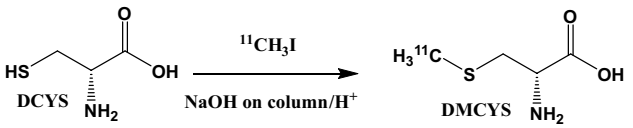

Scheme 1 Radiosynthesis of DMCYS by on-column ^{11}C-methylation

Statistical analysis

All data were expressed as mean ± SD. Statistical analysis was performed with SPSS software, version 17.0 (SPSS Inc.), for Windows (Microsoft). Comparisons between conditions were performed using the unpaired, 2-tailed Student's t test. A p value of less than 0.05 was considered to indicate statistical significance.

Results

Radiosynthesis

Automated synthesis of DMCYS was performed by ^{11}C-methylation of the precursor D-cysteine with $^{11}CH_3I$ (Scheme 1). The uncorrected radiochemical yield of DMCYS from $^{11}CH_3I$ was more than 50 % with a total synthesis time from $^{11}CO_2$ was about 12 min. The radiochemical purity of DMCYS was over 99 % (Fig. 2) and the enantiomeric purity was above 90 %. The retention time was approximately, 3.0–4.0 min for DMCYS, less than 1.5 min for D-cysteine, and approximately, 14.6 min for $^{11}CH_3I$. Similar to MET and LMCYS, a simple, rapid and efficient automated synthesis of DMCYS was provided with high radiochemical yield and high radiochemical purity within a short synthesis time.

Transport mechanism of DMCYS in vitro

The contribution of specific transport systems to DMCYS, MET and LMCYS uptake by measuring their intracellular

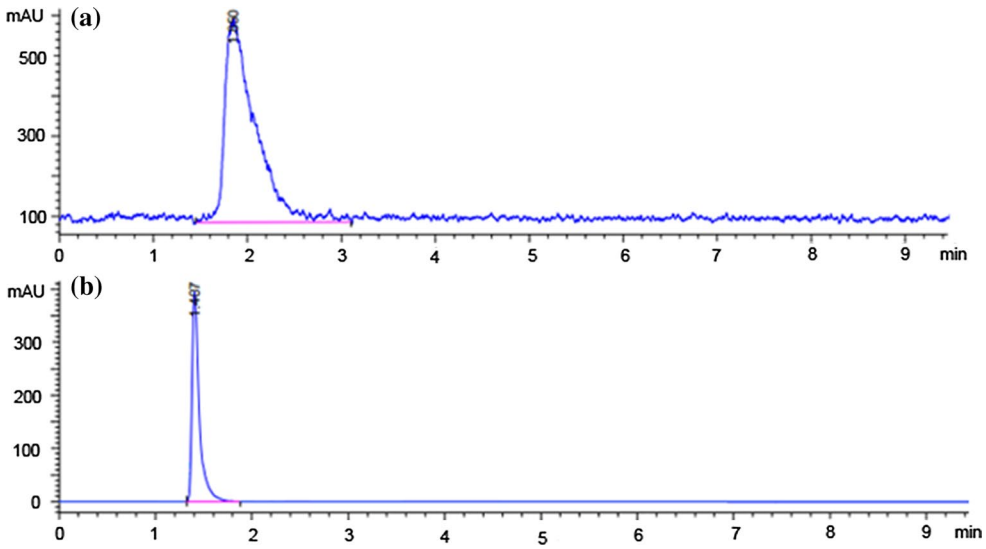

Fig. 2 Typical HPLC chromatograms of DMCYS and the standard coinjection. **a** Radioactive chromatogram of DMCYS. **b** Ultraviolet chromatogram of the standard DMCYS. (mAU: milli absorbance unit)

accumulations in Hepa 1–6 cells in the absence or presence of Na^+ or various types of inhibitors, is shown in Fig. 3. The most conspicuous difference among three ^{11}C-labeled amino acids was observed in the presence of the amino transport system L inhibitor BCH and ASC inhibitor serine. In Na^+-containing buffer, BCH and serine approximately, reduced the uptake of DMCYS by 40 and 46 % ($n = 15$), respectively while BCH inhibited uptake of the tracer by 69 % ($p < 0.01$, $n = 15$) in the replacement of Na^+ by choline. In the presence of the amino acid transport system A inhibitor *N*-methyl-2-amino-isobutyric acid (MeAIB), no significant effect on uptake was shown. Therefore, DMCYS was primarily transported by Na^+-independent L transporter and Na^+-dependent ASC transporter in Hepa 1–6 cells, and mediated mainly by system L and systems ASC, with almost no involvement of systems A.

The transport characteristics of MET and LMCYS were very similar in this cell line. In contrast, addition of BCH resulted in an approximately, 80 % ($p < 0.01$, $n = 15$) reduction of MET and LMCYS uptake in the presence of Na^+, whereas the addition of MeAIB and serine caused almost no significant change ($p = 0.15 > 0.05$) in tracers uptake (Fig. 3a). In the replacement of Na^+ by choline, BCH inhibited uptake of LMET and LMCYS by approximately, 80 % ($p < 0.01$, $n = 15$), and serine slightly decreased uptake of two tracers to approximately, 90 % of the control. In the presence or absence of Na^+, the transport system A inhibitor MeAIB had almost no significant effect on uptake of MET and LMCYS. The results suggested that MET and LMCYS were primarily transported by a specific Na^+-independent transporter in Hepa 1–6 cells and mediated mainly by system L with minor systems A and ASC. Interestingly, BCH is regarded as an inhibitor of the Na^+-independent system L, but also of the Na^+-dependent system $B^{0,+}$ (Sloan and Mager 1999). Thus, DMCYS uptake partly inhibited by BCH in the presence of Na^+, indicating that DMCYS transport could be mediated through Na^+-dependent system $B^{0,+}$. Similar to DMCYS, MET and LMCYS uptake markedly inhibited by BCH in the presence of Na^+, suggested their transport was also mediated through Na^+-dependent system $B^{0,+}$.

The experiments with increasing concentrations of unlabeled DMCYS (0–350 μmol/L) showed no significant change in the radioactivity concentration in the cells (Fig. 3b). No saturation of transport capacity was found until a concentration of 350 μmol/L was reached.

Incorporation of DMCYS into proteins

Samples precipitated with trichloroacetic acid (TCA) after incubation with DMCYS for 30 min, demonstrated less than 1 % of the radioactivity in the acid precipitable fraction similar to LMCYS (Fig. 3c). Therefore, no incorporation of DMCYS into protein could be found.

In vivo biodistribution

The comparison of the biodistribution data of D- and L-isomers of ^{11}C-MCYS in normal mice is summarized

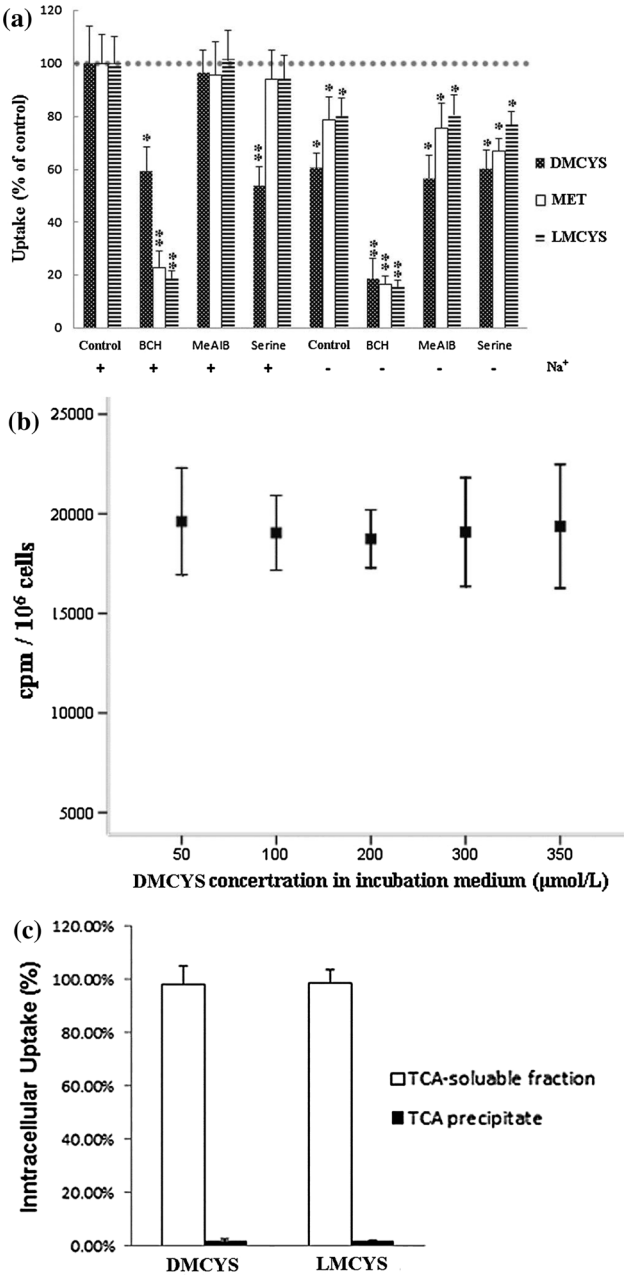

Fig. 3 Comparison of DMCYS, MET and LMCYS uptake by Hepa1–6 cells. **a** Values are given as percentage (mean ± SD, $n = 9$–15) of uptake in cells that were incubated with or without inhibitors including BCH or MeAIB or serine (15 mmol/L) in Na^+-containing (+) or Na^+-absent (−) buffer. *$p < 0.05$. **$p < 0.01$. **b** Uptake of DMCYS per 10^6 cells at different concentrations of DMCYS in incubation medium. **c** Radioactivity accumulation of DMCYS and LMCYS in TCA precipitate and TCA-soluble fractions at 30 min after injection

in Table 1. The biodistribution showed that the uptake of DMCYS in blood was higher than that of LMCYS throughout the study and decreased gradually with time post-injection. The uptake of LMCYS was relatively low and stable in the abdominal organs, whereas the DMCYS revealed much lower uptake and faster clearance compared with the corresponding L-isomers, except in the kidney and liver at the early phase. In contrast, the brain showed slower clearance and lower uptake of DMCYS than those of LMCYS at 15-min after injection. Among the interesting organs, the pancreas demonstrated a remarkably high uptake of two ^{11}C-labeled compounds. However, the D-isomer had faster clearance than the L-isomer in the pancreas.

PET imaging

Whole-body DMCYS PET imaging provided the consistent distribution data (Fig. 4) with those obtained from the tissue dissection assays above. Figure 4 showed PET images of fibrosarcoma-bearing mice and inflammatory mice at 60-min post-injection of DMCYS, LMCYS, MET, and FDG, respectively. High uptakes of DMCYS and FDG (Fig. 4b, h) and relatively low uptakes of LMCYS and LMET (Fig. 4d, f) were found in the inoculated tumors. Similarly, high uptake of FDG was observed in the inflammatory tissue (Fig. 4g). In contrast, low uptakes of DMCYS (Fig. 4a), LMCYS (Fig. 4c) and MET (Fig. 4e) were found in inflammatory tissues.

Figure 4 PET images of tumor-bearing mice (b, d, f, h, yellow arrow) and inflammatory mice (a, c, e, g, white arrow) obtained at 60 min post-injection of DMCYS, LMCYS, MET and ^{18}F-FDG, respectively. The three images in each picture (a–h) were transaxial CT (upper left), transaxial PET (lower left) and maximum intensity projection (MIP, right) PET images, respectively.

The uptake percentages of DMCYS, LMCYS, MET, and FDG in dissected blood, tumor, inflammatory lesion, and muscle at 60-min post-injection are shown in Table 2. FDG had the lowest tumor-to-inflammation (T/I) ratio (blood corrected 1.52, muscle corrected 1.49) among all used PET tracers, which made FDG difficult to differentiate tumor from inflammation. DMCYS, LMCYS, and MET also showed high-uptake in the fibrosarcoma tumor, however, they had low accumulation in inflammation. High tumor-to-inflammation ratio revealed that DMCYS and LMCYS accumulation in tumor was less affected by inflammatory lesion compared with MET and FDG ($p < 0.05$). However, the uptake difference between DMCYS and LMCYS was not significant ($p > 0.05$).

The selectivity (blood) and selectivity (muscle) indices were 2.93 and 2.64 for DMCYS, and 2.05 and 2.13 for LMCYS, respectively, which were higher than those for MET and FDG ($p < 0.05$).

PET images of orthotopic-transplanted brain glioma rat models are shown in Fig. 5. A low uptake of DMCYS was detected in normal brain tissue, but a high uptake in brain glioma tissue was observed. At 30 min post-injection

Table 1 Biodistribution of DMCYS and LMCYS in normal mice after intravenous injection

Organ	Isomer	5 min	15 min	30 min	45 min	60 min
Blood	D	1.12 ± 0.13	0.90 ± 0.10	0.52 ± 0.07	0.51 ± 0.05	0.40 ± 0.06
	L	1.01 ± 0.09	0.73 ± 0.09	0.47 ± 0.07	0.41 ± 0.08	0.29 ± 0.04
Brain	D	0.31 ± 0.05	0.70 ± 0.06	0.47 ± 0.08	0.34 ± 0.03	0.26 ± 0.04
	L	0.82 ± 0.06	0.61 ± 0.09	0.33 ± 0.08	0.19 ± 0.07	0.13 ± 0.05
Heart	D	0.84 ± 0.05	0.65 ± 0.07	0.48 ± 0.09	0.29 ± 0.02	0.16 ± 0.03
	L	0.92 ± 0.15	0.89 ± 0.10	0.64 ± 0.06	0.42 ± 0.05	0.31 ± 0.07
Lung	D	0.80 ± 0.07	1.07 ± 0.15	0.35 ± 0.06	0.27 ± 0.03	0.15 ± 0.02
	L	0.89 ± 0.11	0.74 ± 0.12	0.40 ± 0.30	0.35 ± 0.30	0.27 ± 0.05
Liver	D	2.52 ± 0.28	1.18 ± 0.11	0.96 ± 0.09	0.40 ± 0.04	0.17 ± 0.02
	L	1.77 ± 0.12	1.38 ± 0.11	1.16 ± 0.09	0.86 ± 0.12	0.53 ± 0.14
Pancreas	D	4.17 ± 0.36	2.85 ± 0.22	1.69 ± 0.14	1.28 ± 0.08	1.13 ± 0.13
	L	3.89 ± 0.09	3.12 ± 0.08	2.58 ± 0.08	2.32 ± 0.06	2.29 ± 0.05
Kidney	D	1.06 ± 0.24	0.75 ± 0.06	0.42 ± 0.07	0.27 ± 0.08	0.10 ± 0.01
	L	0.88 ± 0.09	0.62 ± 0.08	0.48 ± 0.08	0.32 ± 0.06	0.29 ± 0.05
Stomach wall	D	0.88 ± 0.27	0.73 ± 0.18	0.54 ± 0.07	0.31 ± 0.04	0.11 ± 0.03
	L	1.09 ± 0.15	0.93 ± 0.10	0.68 ± 0.09	0.44 ± 0.07	0.28 ± 0.04
Small intestine	D	0.87 ± 0.11	0.66 ± 0.08	0.48 ± 0.05	0.33 ± 0.08	0.21 ± 0.05
	L	0.99 ± 0.32	0.73 ± 0.19	0.61 ± 0.23	0.47 ± 0.07	0.35 ± 0.14
Muscle	D	0.51 ± 0.10	0.37 ± 0.06	0.32 ± 0.03	0.27 ± 0.04	0.24 ± 0.03
	L	0.66 ± 0.04	0.52 ± 0.08	0.48 ± 0.05	0.43 ± 0.06	0.38 ± 0.02

Data are expressed as average %ID/g ± SD ($n = 5$ at each time point)

of DMCYS, uptake ratio of glioma tissue to white matter and glioma tissue to gray matter was 3.00 ± 0.56 and 1.82 ± 0.35, respectively, which was a little higher than that at 60-min post-injection of FDG (2.17 ± 0.21 and 1.42 ± 0.17, respectively). The results demonstrated that DMCYS was a useful PET tracer for brain cancer imaging.

Discussion

Generally, LMCYS is a naturally occurring inexpensive water-soluble compound with antioxidative and anti-inflammatory properties and no adverse effects and exists abundantly in some routine food (Deng et al. 2011). Our previous study showed that LMCYS was a potential amino acid PET tracer for the differentiation of tumor from inflammation (Deng et al. 2011). In this study, radiosynthesis and evaluation of D-isomer of ^{11}C-MCYS as a potential tumor-imaging agent were performed in comparison with its corresponding L-isomer. Similar to LMCYS, a simple, rapid, and efficient automated synthesis of DMCYS was provided with high radiochemical yield and high radiochemical purity within a short synthesis time.

In general, the tumor uptake is thought to reflect the increased amino acid transport and the protein synthesis. As we expected, DMCYS was primarily taken up into the acid-soluble amino acid pool and not into the acid-precipitable protein fraction, which was consistent with other D-isomeric amino acid analogs, such as DFET, DFMT, and DFPHCys (Denoyer et al. 2012; Tsukada et al. 2006a, b). DMCYS showed almost no incorporation into the protein fraction similar to the corresponding L-isomers (Deng et al. 2011), but in contrast to MET with partly incorporated into protein. The results strongly suggested that the uptake of DMCYS in tumor could predominantly reflect the amino acid transport rather than protein incorporation.

Most amino acids are taken up via members of three plasma membrane transporter families, designated as sodium-independent system L (leucine-preferring), sodium-dependent system A (alanine-preferring) and system ASC (alanine, serine, cysteine transport). Our transport experiments showed that LMCYS, like MET, was primarily transported by a specific Na^+-independent transporter in Hepa 1–6 cells and mediated mainly by system L with almost no systems A and ASC, which was consistent with the reported results (Deng et al. 2011; Jager et al. 2001). Also, our competitive inhibition assays clearly demonstrated DMCYS transport in Hepa 1–6 cells consisted of two processes, a saturable Na^+-dependent activities and a non-saturable sodium-independent route. Interestingly, BCH is regarded as an inhibitor of the Na^+-independent system L, but also of the Na^+-dependent system $B^{0,+}$ (Sloan and Mager 1999). Thus, DMCYS uptake partly inhibited by BCH in the presence of Na^+, indicating that DMCYS transport could be mediated through Na^+-dependent system $B^{0,+}$. Similar to DMCYS, MET and LMCYS uptake markedly inhibited by BCH, suggested that their transport was also mediated through Na^+-dependent system $B^{0,+}$. In addition, in the presence of Na^+, serine also partly inhibited DMCYS uptake via system ASC. Moreover, in the absence of Na^+, the accumulation of DMCYS was mainly inhibited by BCH, while MeAIB, serine, and MCYS did not inhibit the uptake of DMCYS. Therefore, DMCYS uptake was primarily transported through the Na^+-independent system L, and also the Na^+-dependent system $B^{0,+}$ and system ASC, with almost no system A.

In the PET and dissection studies, FDG showed significantly high accumulation in both tumor and inflammatory lesion, resulting in low tumor-to-inflammation ratio of 1.40 at 60-min post-injection. MET also exhibited low tumor-to-inflammation ratio of 1.64 because of low uptake in both tumor and inflammatory lesion. By contrast, DMCYS showed moderate accumulation in tumor and very low uptake in inflammatory lesion, leading to relatively higher

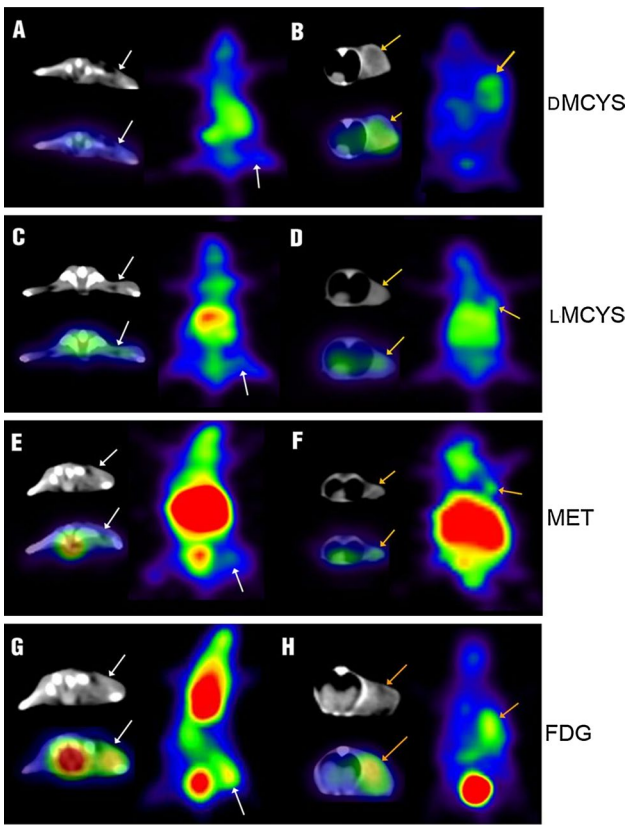

Fig. 4 PET images of tumor-bearing mice (**b**, **d**, **f**, **h**, *yellow arrow*) and inflammatory mice (**a**, **c**, **e**, **g**, *white arrow*) post-injection of DMCYS, LMCYS, MET and FDG, respectively. The three images in each picture (**a**–**h**) were transaxial CT (*upper left*), transaxial PET (*lower left*) and maximum intensity projection (MIP, right) PET images, respectively

Table 2 Radioactivity accumulation in blood, tumor, inflammatory lesion and muscle derived from PET images of fibrosarcoma-bearing mice and inflammatory mice at 60 min post-injection of DMCYS, LMCYS, MET and FDG

Tissue	DMCYS	LMCYS	MET	FDG
Blood	0.40 ± 0.06	0.29 ± 0.04	0.43 ± 0.03	0.81 ± 0.15
Tumor	2.54 ± 0.35	2.83 ± 0.27	2.45 ± 0.49	5.31 ± 0.36
Inflammation	1.13 ± 0.29	1.53 ± 0.15	1.49 ± 0.37	3.78 ± 1.11
Muscle	0.27 ± 0.03	0.38 ± 0.03	0.53 ± 0.08	0.64 ± 0.11
Tumor-to-blood ratio	6.35	9.76	5.70	6.56
Tumor-to-muscle ratio	9.41	7.45	4.62	8.30
Inflammation-to-blood ratio	2.83	5.28	3.47	4.67
Inflammation-to-muscle ratio	4.19	4.03	2.81	5.91
Tumor-to-inflammation ratio	2.25	1.85	1.64	1.40
Selectivity(blood)[a]	2.93	2.05	1.91	1.52
Selectivity(muscle)[a]	2.64	2.13	2.00	1.49

Mice ($n = 5$ per each tracer) were injected intravenously with labeled tracers via tail vein and sacrificed at 60 min after injection; tissue samples were rapidly removed, and weight and radioactivity were measured. Data in blood, tumor, muscle, and inflammatory tissue are expressed as average %ID/g ± SD

[a] Defined as (tumor uptake−blood or muscle uptake)/(inflammation uptake−blood or muscle uptake)

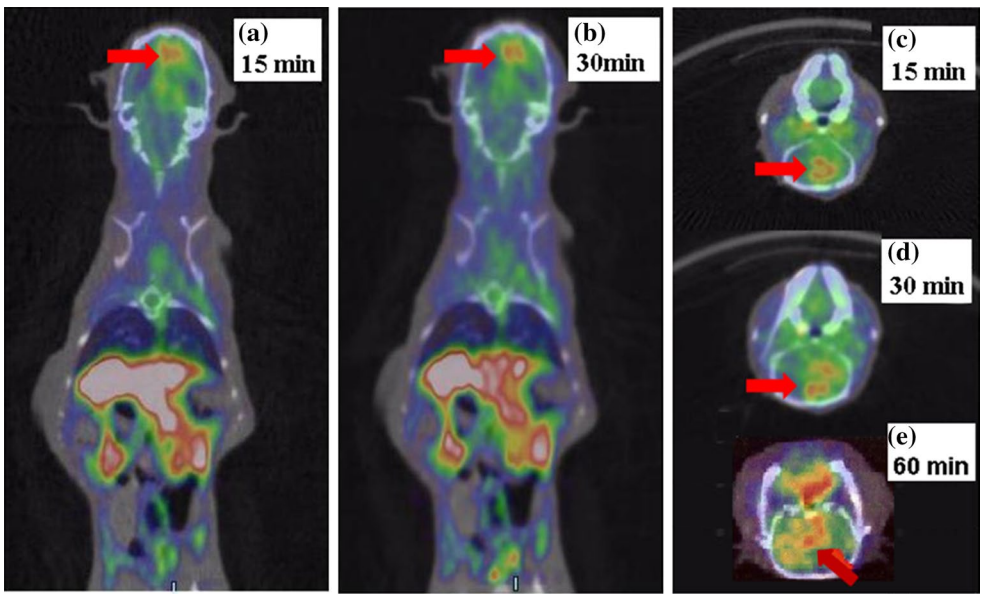

Fig. 5 PET images of orthotopic transplanted C6 brain glioma model rats at 15 min (**a**, **c**) and 30 min (**b**, **d**) post-injection of DMCYS and 60 min post-injection of FDG (**e**). **a** and **b**, coronal PET-CT fused images; **c**, **d** and **e**, transaxial PET-CT fused images

tumor-to-inflammation ratio of 2.25 than LMCYS (1.85) at 60 min post-injection (Table 2), which was possibly contributed to their different amino acid transport mechanism. Moreover, DMCYS demonstrated the highest selectivity indices (blood corrected 2.93, muscle corrected 2.64) among the four tracers. Almost no uptake of DMCYS in inflammatory lesion could be related to very low protein incorporation. The biodistribution demonstrated higher uptake of DMCYS in pancreas and liver at 5-min post-injection, relatively lower uptake in brain and muscle during the entire observation time, and faster radioactivity clearance from most tissues than those of L-isomer. In addition, PET images of orthotopic transplanted glioma models showed low uptake of DMCYS in normal brain tissue and high uptake in glioma tissue. Thus, rapid clearance and low accumulation of DMCYS in most tissues, and high tumor-to-inflammation ratio indicate that DMCYS may be a useful amino acid tracer for PET imaging of cerebral and peripheral tumors.

Conclusion

In summary, the study demonstrated that DMCYS was very easy to perform the automated synthesis and seemed to be

more potential for tumor imaging than the corresponding L-isomers (LMCYS). DMCYS uptake was primarily transported through Na^+-independent system L, Na^+-dependent system $B^{0,+}$ and system ASC, with almost no system A. Like LMCYS, DMCYS was not incorporated into proteins. High tumor-to-inflammation ratio showed DMCYS was superior to MET and FDG in the differentiation of tumor from inflammation. The results suggest that DMCYS has the potential to identify highly metabolically active tumors and may in turn improve the management of patients by monitoring tumor progression, but further confirmation is needed in clinical studies.

Acknowledgments This work was supported in part by the Science and Technology Foundation of Guangdong Province (No. 2010B031600054), the National High Technology Research and Development Program of China (863 Program, No. 2008AA02Z430), the National Natural Science Foundation of China (No. 81371584), Science and Technology Planning Project of Guangzhou (2011J5200025), and Doctoral Candidate Innovative Personnel Training Project of Sun Yat-Sen University (2012).

Conflict of interest The authors declare that they have no conflict of interest.

References

Bourdier T, Shepherd R, Berghofer P, Jackson T, Fookes CJ, Denoyer D, Dorow DS, Greguric I, Gregoire MC, Hicks RJ, Katsifis A (2011) Radiosynthesis and biological evaluation of L- and D-*S*-(3-[^{18}F]fluoropropyl)homocysteine for tumor imaging using positron emission tomography. J Med Chem 54:860–1870

Deng H, Tang X, Wang H, Tang G, Wen F, Shi X, Yi C, Wu K, Meng Q (2011) *S*-^{11}C-methyl-L-cysteine: a new amino acid PET tracer for cancer imaging. J Nucl Med 52:287–293

Denoyer D, Kirby L, Waldeck K, Roselt P, Neels OC, Bourdier T, Shepherd R, Katsifis A, Hicks RJ (2012) Preclinical characterization of ^{18}F-D-FPHCys, a new amino acid-based PET tracer. Eur J Nucl Med Mol Imaging 39:703–712

Hamacher K, Coenen HH (2002) Efficient routine production of the ^{18}F-labelled amino acid *O*-2-^{18}F fluoroethyl-L-tyrosine. Appl Radiat Isot 57:853–856

Jager PL, Vaalburg W, Pruim J, de Vries EG, Langen KJ, Piers DA (2001) Radiolabeled amino acids: basic aspects and clinical applications in oncology. J Nucl Med 42:432–445

Kubota K (2001) From tumor biology to clinical PET: a review of positron emission tomography (PET) in oncology. Ann Nucl Med 15:471–486

Kubota R, Kubota K, Yamada S, Tada M, Ido T, Tamahashi N (1994) Microautoradiographic study for the differentiation of intratumoral macrophages, granulation tissues and cancer cells by the dynamics of fluorine-18-fluorodeoxyglucose uptake. J Nucl Med 35:104–112

Kumar R, Halanaik D, Malhotra A (2010) Clinical applications of positron emission tomography-computed tomography in oncology. Indian J Cancer 47:100–119

Langen KJ, Muhlensiepen H, Schmieder S, Hamacher K, Broer S, Borner AR, Schneeweiss FH, Coenen HH (2002) Transport of *cis*- and *trans*-4-[(^{18})F]fluoro-L-proline in F98 glioma cells. Nucl Med Biol 29:685–692

Langen KJ, Jarosch M, Muhlensiepen H, Hamacher K, Broer S, Jansen P, Zilles K, Coenen HH (2003) Comparison of fluorotyrosines and methionine uptake in F98 rat gliomas. Nucl Med Biol 30:501–508

Langstrom B, Antoni G, Gullberg P, Halldin C, Malmborg P, Nagren K, Rimland A, Svard H (1987) Synthesis of L- and D-[methyl-^{11}C]methionine. J Nucl Med 28:1037–1040

Lee TS, Ahn SH, Moon BS, Chun KS, Kang JH, Cheon GJ, Choi CW, Lim SM (2009) Comparison of ^{18}F-FDG, ^{18}F-FET and ^{18}F-FLT for differentiation between tumor and inflammation in rats. Nucl Med Biol 36:681–686

Maeda Y, Oguni H, Saitou Y, Mutoh A, Imai K, Osawa M, Fukuyama Y, Hori T, Yamane F, Kubo O, Ishii K, Ishiwata K (2003) Rasmussen syndrome: multifocal spread of inflammation suggested from MRI and PET findings. Epilepsia 44:1118–1121

Nunez R, Macapinlac HA, Yeung HW, Akhurst T, Cai S, Osman I, Gonen M, Riedel E, Scher HI, Larson SM (2002) Combined ^{18}F-FDG and ^{11}C-methionine PET scans in patients with newly progressive metastatic prostate cancer. J Nucl Med 43:46–55

Okubo S, Zhen HN, Kawai N, Nishiyama Y, Haba R, Tamiya T (2010) Correlation of L-methyl-^{11}C-methionine (MET) uptake with L-type amino acid transporter 1 in human gliomas. J Neurooncol 99:217–225

Pascali C, Bogni A, Iwata R, Decise D, Crippa F, Bombardieri E (1999) High efficiency preparation of L-[*S*-methyl-^{11}C]methionine by on-column [^{11}C]methylation on C18 Sep-Pak. J Labelled Compds Radiopharm 42:715–724

Plathow C, Weber WA (2008) Tumor cell metabolism imaging. J Nucl Med 49(Suppl 2):43S–63S

Sasaki M, Kuwabara Y, Yoshida T, Nakagawa M, Koga H, Hayashi K, Kaneko K, Chen T, Ichiya Y, Masuda K (2001) Comparison of MET-PET and FDG-PET for differentiation between benign lesions and malignant tumors of the lung. Ann Nucl Med 15:425–431

Sloan JL, Mager S (1999) Cloning and functional expression of a human Na^+ and Cl^- dependent neutral and cationic amino acid transporter $B^{0,+}$. J Biol Chem 274:23740–23745

Tang GH, Wang MF, Tang XL, Luo L, Gan MQ (2004) Automated synthesis of (*S*-[^{11}C]-methyl)-L-methionine and (*S*-[^{11}C]-methyl)-L-cysteine by on-column [^{11}C]methylation. J Nucl Radiochem 26:77–83

Tang GH, Tang XL, Wang MF, Guo XJ (2006) High efficient automated synthesis of 2-[^{18}F]-fluoro-2-deoxy-D-glucose. Nucl Technol 29:531–536

Tsukada H, Sato K, Fukumoto D, Kakiuchi T (2006a) Evaluation of D-isomers of *O*-^{18}F-fluoromethyl, *O*-^{18}F-fluoroethyl and *O*-^{18}F-fluoropropyl tyrosine as tumour imaging agents in mice. Eur J Nucl Med Mol Imaging 33:1017–1024

Tsukada H, Sato K, Fukumoto D, Nishiyama S, Harada N, Kakiuchi T (2006b) Evaluation of D-isomers of *O*-^{11}C-methyl tyrosine and *O*-^{18}F-fluoromethyl tyrosine as tumor-imaging agents in tumor-bearing mice: comparison with L- and D-^{11}C-methionine. J Nucl Med 47:679–688

Urakami T, Sakai K, Asai T, Fukumoto D, Tsukada H, Oku N (2009) Evaluation of *O*-[^{18}F]fluoromethyl-D-tyrosine as a radiotracer for tumor imaging with positron emission tomography. Nucl Med Biol 36:295–303

Yamada S, Kubota K, Kubota R, Ido T, Tamahashi N (1995) High accumulation of fluorine-18-fluorodeoxyglucose in turpentine-induced inflammatory tissue. J Nucl Med 36:1301–1306

Yasukawa T, Yoshikawa K, Aoyagi H, Yamamoto N, Tamura K, Suzuki K, Tsujii H, Murata H, Sasaki Y, Fujisawa T (2000) Usefulness of PET with ^{11}C-methionine for the detection of hilar and mediastinal lymph node metastasis in lung cancer. J Nucl Med 41:283–290